Available online at www.sciencedirect.com
ScienceDirect
Composites Science and Technology xxx (2007) xxx–xxx
COMPOSITES SCIENCE AND TECHNOLOGY
www.elsevier.com/locate/compscitech

Experimental methodology of study of damage initiation and development in textile composites in uniaxial tensile test

S.V. Lomov *, D.S. Ivanov, T.C. Truong, I. Verpoest, F. Baudry, K. Vanden Bosche, H. Xie

Department of Metallurgy and Materials Engineering, Katholieke Universiteit Leuven, Kasteelpark Arenberg, 44, B-3001 Leuven, Belgium

Received 27 April 2007; received in revised form 4 July 2007; accepted 5 July 2007

Abstract

Damage in textile composites is closely connected with the internal micro- and meso-geometry of the reinforcement, and reveals features, which are not present in the damage processes in classical laminates. This paper proposes a test sequence intended to characterise damage in textile composites – its initiation and development different scale levels: (1) Tensile tests on samples cut in characteristic directions of the textile reinforcement (machine, cross and bias), accompanied with acoustic emission (AE) registration and full-field strain measurement on the surface. The test produces stress–strain diagrams and identifies characteristic strain levels for post-mortem investigation: just after first damage ε_1; well-developed damage ε_2; just before the final fracture of the sample ε_3. Full-field strain measurement highlights the relation between strain concentrations (linked with the damage initiation) and the reinforcement structure. (2) Samples loaded up to $\varepsilon_{1\ldots3}$ are examined with CT and X-ray. This reveals the damage pattern and allows quantitative characterising of the damage development. (3) Optical and SEM examination of cross-sections through the damage sites, determined with X-ray, identifies local damage modes. The same strain levels are further used for setting up fatigue tests. The experimental protocol is applied for triaxial braided and quasi-UD composites.

Keywords: A. Textile composites; B. Strength; B. Stress–strain curves; D. Acoustic emission

1. Introduction

Textile composites are steadily gaining positions in aeronautic, automotive, ground transportation and other applications, offering weight reductions over metal alternative and cost saving against lay-up of UD tapes. Whilst the design for stiffness of textile composite parts can use validated predictive modelling, related to the meso-structure of textile reinforcements [1–5], the reliable design for strength with not-that-exaggerated safety factors has to be based mostly on empirical information, with modelling approaches being developed [1,6–11], but still have not reached a mature state. Validation of the modelling methods asks for adequate experimental characterisation of the damage processes on different scale and hierarchical levels of the composite, as the damage phenomena in textile composites are much more complicated then in UD laminates, and involves processes and parameters on different scale levels: macro (overall strength and strain-to failure of the sample and stiffness reduction), meso (damage initiation sites inside the textile structure of the reinforcement) and micro (local damage mode inside yarns and fibrous plies).

Tensile loading of the test sample is one of the most common testing procedures. It ensures well-controlled plane stress–strain state of the sample and the set-up allows easy monitoring of the deformations of the sample with full-field optical strain measurement on the sample surface and of damage phenomena – with acoustic emission. During a tensile test, the macro stress–strain field in the centre of the sample is reasonably homogeneous, if the width of the sample is about several times the size of the unit cell of the textile composite. The macro-scale phenomena, as peculiarities of the stress–strain fields near the grips, are

* Corresponding author. Tel.: +32 16 32 12 10; fax: +32 16 32 19 90.
E-mail address: Stepan.Lomov@mtm.kuleuven.be (S.V. Lomov).

0266-3538/$ - see front matter © 2007 Elsevier Ltd. All rights reserved.
doi:10.1016/j.compscitech.2007.07.005

considered rather as complications for the processing of the experimental data. Attention is drawn to the homogenised performance of the material and to meso-scale phenomena.of damage initiation and development. The processes on the meso-level can be monitored during the test or damage can be studied "post-mortem" with optical or X-ray inspection. The post-mortem examination can go further to SEM to study the details of fibre debonding. Tension-induced damage in textile composites was reported in a number of publications.

1.1. Woven composites

John et al. [12] have presented a "taxonomy" of damage for complex combination of longitudinal, transverse cracks and delamination in 3D woven fabric. Development of damage is linked to the change of the sample stiffness, and microstructure of cracks is studied on cross-sections using optical microscopy. The damage starts with transversal cracking, which lead to appearance of longitudinal cracks and subsequent debonding on the boundaries impregnated yarn–matrix. The latter was also observed to be the damage initiation mechanism in 3D woven carbon/epoxy fabrics [13]. These features, complexly linked in 3D woven composites, are evident also in 2D woven laminates, as studied in [9,14–16]. These authors register damage using mainly cross-sectioning and optical microscopy; Sugimoto et al. [16] used acoustic emission (AE) for detection of the damage onset. In all these studies, the load is applied in the direction of warp or weft yarns.

1.2. Braided composites

Masters and Ifju [17] studied the initiation and development of damage in three-axial braided composites in tension using AE combined with Moire interferometry during the test and X-ray and optical microscopy post-mortem examination of the samples. Initiation of transversal cracking progressing to delamination and complete failure of the sample is monitored. Even when the loading is applied in the direction of one of the yarn systems, other yarns in a three-axial braid go in bias directions; nevertheless the development of damage follows the same sequence as in woven (orthogonal) composites. Damage development in braided composites was further studied in the work of the present authors [11,18–20], using the methodology discussed in the present paper.

1.3. Non-crimp fabric (NCF) composites

Damage patterns in non-crimp fabric reinforced composites was studied in [10,21–25]. Edgren et al. [21] has classified the types of cracks in relation to the internal geometry of 0/90 NCF [25] and discussed the development of the damage modes. The studies of Truong et al. [22,23,26] cover more diverse structures of NCF (0/90, ±45, 0/ + 45/90/45). Using the methodology, presented here, the initiation and development of damage is monitored and described. NCF composites exhibit the same damage onset scenario, namely transversal cracks in the fibre bundles, as in woven and braided composites. The difference is in the crack length: in NCF the cracks can easily propagate along the fibre bundles. The transverse cracks are followed by local delaminations, which may lead to the curious and not fully explained premature fibre damage in NCF composites as observed by Mattsson et al. [27]. The studies [22,23] cover also tensile loading in the off-axis direction for biaxial NCF and damage in composites made of sheared reinforcements, lately also studied in [10].

Summarising the findings of the cited research, the following damage phenomena in textile composites can be identified during tensile loading:

- Pre-existing damage induced by the composite processing (thermal and cure stresses).
- Damage initiation, normally by transverse cracking of the fibre bundles, sometimes by cracking along the boundaries of the bundles (started by debonding on the scale of individual fibres).
- Damage propagation and associated reduction of the material stiffness: (1) grow and stoppage of cracks; (2) multiplication of cracks; and (3) correlation with the reinforcement architecture.
- Local delaminations and debonding (on the scale of yarn/matrix interface).
- Fibre damage and sample failure.

The aim of the paper is to describe a methodology of a systematic study of these phenomena during tensile deformation of textile composites. The proposed experimental protocol is illustrated on two cases of carbon/epoxy composite, reinforced with triaxial braid and quasi-UD fabric. A thorough study of damage in NCF composites, performed using the proposed methodology, can be found in [22,23,26].

2. Tensile test, damage monitoring and post-mortem characterisation

The proposed suite of tests includes:

- Tensile test with acoustic emission (AE) and full-field strain mapping (SM).
- X-ray and ultrasonic C-scan examination of the samples after tension up to certain strain levels, identified by AE and SM results.
- Cross-sectioning and microscopical examination of the samples in the places defined by the X-ray examination.

2.1. Tensile test

Tensile test is done on a standard testing machine (here: Instron 4505, test speed 1 mm/min). The samples are cut

Please cite this article in press as: Lomov SV et al., Experimental methodology of study of damage initiation ..., Compos Sci Technol (2007), doi:10.1016/j.compscitech.2007.07.005

out of the composite plates in the characteristic directions dictated by the textile structure: (1) test in the direction of one of the yarn systems of the textile (warp/weft for woven fabrics; braiding/inlay yarns for braids); and (2) test in the direction transversal or bias to the direction of the yarn systems in the textile (bias for woven fabrics, perpendicular to the production direction for braids). In literature damage in textile composites is often studied only for the fibre direction, which does not give the full picture.

2.2. Acoustic emission

Acoustic emission (AE) is defined by [28] as the detection of transient stress waves propagating in a material that are the result of a fast release of strain energy in that material. In the tensile test setup described here, two AE sensors are used situated at the boundaries of the gauge length region. The sensors have to be removed before ultimate failure of the sample to avoid possible damage to them. To calibrate the AE sensors, the ''pencil test'' technique is used: the lead of a 2H pencil is broken on the sample surface on the ''grip side'' of each sensor (that is, between the AE sensor and the grips of the tensile tester). By knowing the distance between the two sensors and the difference in time that the single signal travelled from one sensor to the other, the velocity of sound within the material can be calculated. In this way, signals that occur outside of the sensors can be filtered out. This procedure must be repeated for each sample orientation due to the highly anisotropic nature of the samples.

The energy of AE events is registered and the dependency *cumulative energy of AE events* vs. *tensile strain* is produced. Changes of rate of generation of AE events, reflected by the change of slope of the diagram, indicate change in damage mechanisms in the sample, as discussed further in the paper. It would be highly desirable to be able to use energy levels of AE events to identify the mode of the damage event caused them, as it is done in [29] for glass/epoxy composites in DCB test. However, the AE event energy level for a given damage event depends on the physical nature of the fibres and the matrix, and in the absence of the verified data the calibration of the data is not feasible.

2.3. Strain mapping

Strain mapping is a system of measuring strain using digital images taken of a sample during loading. To achieve better image recognition by the software, the samples are first painted with a black and white random speckle pattern to give a unique pattern of the examined surface. These unique patterns can then be identified by the strain mapping software program. Changes in the displacement of the speckle dots can be identified to quantify the deformation of the sample (the speckle pattern deforms with the sample under loading). As the tensile test proceeds, the system takes subsequent images and analyses them in comparison to either the initial image or the previous image and determining local displacement and strain values. For textile composites, the stress and strain values may vary significantly over the pattern of weaving, braiding or knitting. Apart from producing a strain field, local strain values can be averaged over the area of interest on the sample (normally a square centre of the sample, full width of it) and global strain levels can be computed, hence the strain mapping system is used also as an optical extensometer, with a precision of about 0.01% strain. Full-field measurements of strain fields and damage identification in textile composites are studied in detail in [19] and are not discussed in this paper.

2.4. X-ray, ultrasonic C-scan and microscopy

The AE and SM registration during the tensile test allows identifying the characteristic applied strain levels for damage onset or change of the damage mode. In subsequent tests, the tensile test stops at these strain levels, and the sample is examined using X-ray and ultrasonic C-scan. The aim of X-ray investigation is detecting very fine matrix cracks that occur within the yarns. An X-ray opaque penetrant (Diiodomethane) is used to fill the cracks and make the contrast higher (only cracks and defects that are connected in some way to the surface can be seen). Ultrasonic C-scan test is more ''rough'' then X-ray, but it is useful for characterisation of the overall damage extent and in revealing overall damage pattern, related to the underlying textile reinforcement structure in the composite. Ultrasonic C-scan studies were previously reported in [22] and are not further discussed here. Finally, having identified the positions of the cracks in the sample, cutting and polishing is done to study a fine structure of the damage inside the sample using optical and electron microscopy. The sites and direction for the cuts are determined using X-ray images of the particular sample.

3. Materials

The materials used as examples of application of the proposed experimental methodology are shown in Table 1 and Fig. 1.

3.1. Triaxial braided carbon/epoxy composites

Braiding yarns in the triaxial braided fabric are organised in a so-called diamond pattern 1/1 (Fig. 1a). If the orientation of inlay yarns (''machine'' direction) is chosen as 0°, then the braiding yarns are directed as ±45°. Note the uneven placement of the braiding yarns, which produces large open regions in the fabric. The tensile tests were performed in machine direction (MD), bias direction (BD) and cross direction (CD), as indicated in Fig. 1a. From six to ten tests were performed for each direction.

Please cite this article in press as: Lomov SV et al., Experimental methodology of study of damage initiation ..., Compos Sci Technol (2007), doi:10.1016/j.compscitech.2007.07.005

Table 1
Parameters of the textile reinforcements, matrices and the composites

Fabric type	Triaxial braid	Quasi-UD woven
Fibres	Carbon T700	Carbon T400 /glass EC5
Yarns	24 K	6 K/n.a.
Linear density, tex	1600	400/22
Thickness, mm,	variable	$0.311 \pm 0.011/0.058 \pm 0.012$
Width, mm	$4.21 \pm 0.21/3.75 \pm 0.16$	$1.58 \pm 0.12/0.62 \pm 0.04$
Fabric	*Fig. 2a*	*Fig. 2b*
Spacing between yarn centre lines, mm	5.03 ± 0.24; $9.25 \pm 0.03/20$	$1.53 \pm 0.10/3.27 \pm 0.06$
Areal density, g/m^2	600	285
Matrix	*Epoxy*	
Young modulus, GPa	2.7	
Poisson coefficient	0.4	
Strength, MPa	70	
Composite tensile specimens	*Produced using RTM*	
Number of layers	4	10
Thickness, mm	3.09 ± 0.06	3.5
Width × length between the grips, mm	40×250	15×200
Fibre volume fraction, %	44 ± 1	46.3

Figures with "/" in column 2 designate data for braiding/inlay yarns; figures with "/" in column 3 designate data for warp/weft yarns.

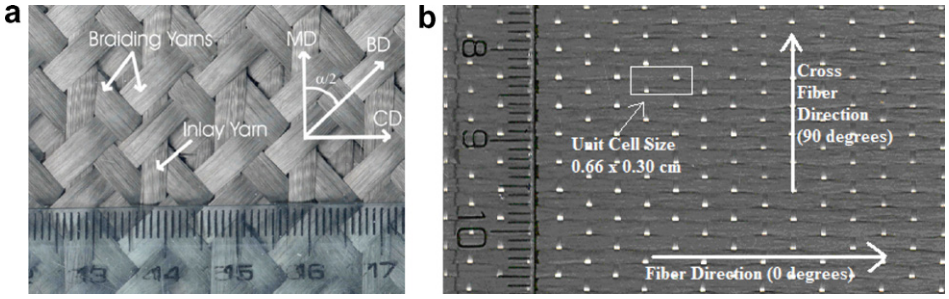

Fig. 1. Textile reinforcements: (a) triaxial braid; (b) quasi-UD woven fabric.

3.2. Quasi-UD woven fabric

The textile used for this study is a quasi-UD fabric from CRAMER GmbH and CO. KG. It is produced by weaving flat UD carbon yarns (warp) with sparse, flat, thin glass yarns (weft). The result is an unbalanced plain weave material. This procedure reduces crimp as much as possible for the warp, however, there is still some crimp of the carbon yarns, which are inclined to the fabric plane in average by an angle of 3.8°. The tensile tests were performed in the directions 0°, 30°, 45°, 60° and 90°, 0° being the direction of the warp carbon yarns (Fig. 1b). From five to seven tests were performed in each direction.

4. Damage initiation: characteristic strain levels

When damage is characterised inside a composite by "post-mortem" study of the sample, it is important that the expected damage condition of the sample when the test is stopped, is well identified. Based on the studies of damage in textile composites, cited in the Introduction, the following stages of the damage development and the correspondent levels of the applied load (strain) can be introduced (Fig. 2):

- onset of transverse cracks (inter-fibre, intra-yarn failure);
- onset of delamination on the boundaries of the fibre bundles;
- onset of fibre failure, starting at delamination, the ultimate failure of the sample.

Note that damage does not necessarily starts with transverse cracking. It may start with localized cracks on the boundaries of the fibre bundles (as observed in 3D carbon/epoxy composites [13]).

This classification could be refined [29], but we propose to keep these three levels as reference points of the damage investigation. An important difficulty is definition what exactly "the damage initiation" means. As the inter-fibre transversal cracks may be created by coalescence of the "crescent" debonding on the individual fibres, the definition of "initiation" is rather fuzzy. We consider the damage initiation strain to be an indication of appearance of a crack, which connects several debonded fibres. In reality such a transversal crack develops fast into a crack through the whole thickness of the yarn.

Fig. 3 shows stress–strain diagrams of two types of composites together with diagrams of cumulative energy of AE events. At the very beginning of the test, few events of low

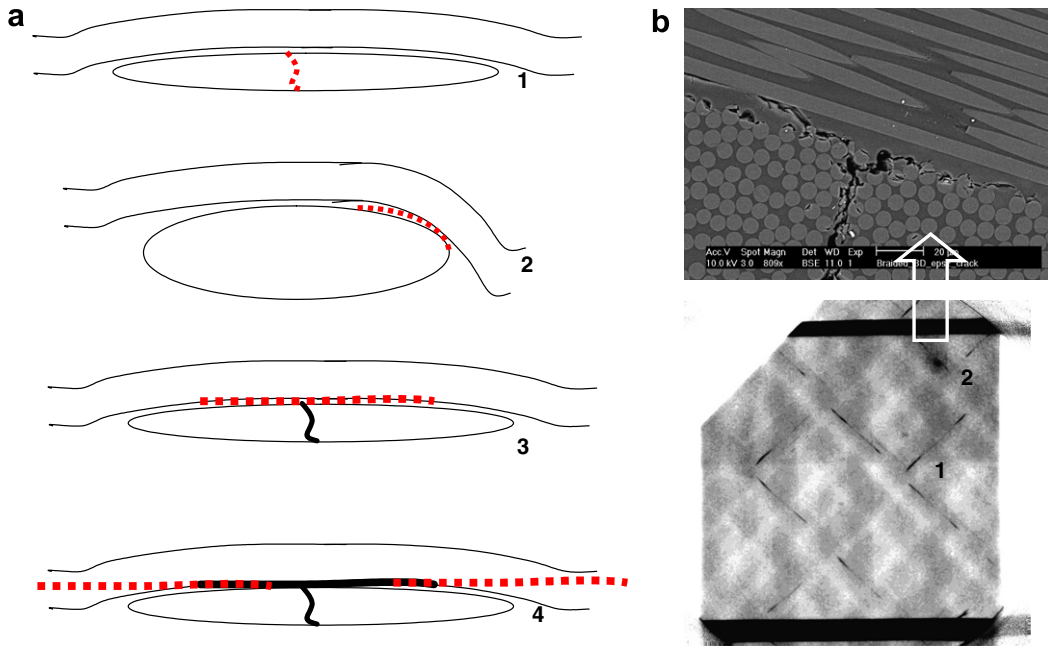

Fig. 2. Characteristic strain levels of damage development: (a) scheme 1 – initiation of a transversal crack, 2 – initiation of micro-delamination between the yarns, 3 – micro-delamination caused by a transversal crack, 4 – delamination causes fibre breakage; (b) X-ray (below) and SEM (above) images, corresponding to the case 3, triaxial braided composite: 1 – transversal cracks, 2 – micro-delamination.

energy contents occur with low frequency. Then the frequency of events increases sharply and the energy content reaches higher levels. This is reflected by the increase of the slope of the cumulative AE event energy curve, which was negligent before. The corresponding *first transition strain* is calculated by the best fit of the bilinear curve (zero before the transition and linearly increasing after it) to the AE cumulative energy diagram. We will designate this first transition strain ε_1. The AE events "heard" before could be interpreted as micro-debonding events; the onset of steady generation of higher energy AE events – as appearance of transversal inter-fibre cracks (triaxial braid) or delaminations on the boundaries glass/carbon yarns (quasi-UD woven).

For triaxial braid, this interpretation is confirmed by X-ray observation of the samples loaded to a strain just below the first transition strain and after it (Fig. 3a). X-ray images reveal no cracks before the transition and appearance of few cracks just after it, which further multiply with the increase of the strain. For quasi-UD woven fabric X-ray examination does not reveal any cracks as they are not connected with the surface of the samples; the damage initiation, detected by AE, was confirmed by microscopical examinations.

For the loading in fibre direction (Fig. 3a), the damage initiation does not affect the slope of the stress–strain diagram, as the resistance to the deformation in fibre direction is provided by the corresponding fibre system (inlay 0° yarns). For the loading in an off-axis direction (Fig. 3b), initiation of damage also corresponds to the transition from the initial linear part of the stress–strain diagram to the non-linear behaviour (Fig. 3b).

After the initiation strain ε_1, the damage behaviour is characterised by constant increase of AE events in the same energy range, giving a steady slope or a "jump" to the cumulative energy curve. This region covers a wide range of strain, until high deformations. At a certain moment, a second "knee" on the AE cumulative energy curve may appear. The corresponding *second transition strain* ε_2 can be again identified by fitting a bilinear curve to the AE cumulative energy diagram. The second transition strain is not that clearly determined as the first. For the case of triaxial braid X-ray observations allow identifying it with the onset of local delaminations (Fig. 3a).

Finally, fibre breakage (loading in fibre direction, Fig. 3a) is indicated by the appearance of extremely high-energy AE events and sharp rise of the cumulative AE events diagram. This happens very close to the final failure of the specimen.

Formal calculation of the transition strains ε_1 and ε_2 (if the second transition on the AE curve exists) is performed by the least square fit of all the cumulative AE energy (CAE) data points (ε_k, CAE_k) by a bilinear function

$$\mathrm{CAE}(\varepsilon;\varepsilon_1,\varepsilon_2,\mathrm{CAE}_1,\mathrm{CAE}_2)=\begin{cases}0,\varepsilon<\varepsilon_1\\(\varepsilon-\varepsilon_1)\cdot\frac{\mathrm{CAE}_1}{\varepsilon_2-\varepsilon_1},\varepsilon_1\leqslant\varepsilon\leqslant\varepsilon_2\\\mathrm{CAE}_1+(\varepsilon-\varepsilon_2)\cdot\frac{\mathrm{CAE}_2-\mathrm{CAE}_1}{\varepsilon_{\max}-\varepsilon_2},\varepsilon>\varepsilon_2\end{cases}$$

with fitting parameters ε_1,ε_2,CAE_1, CAE_2.

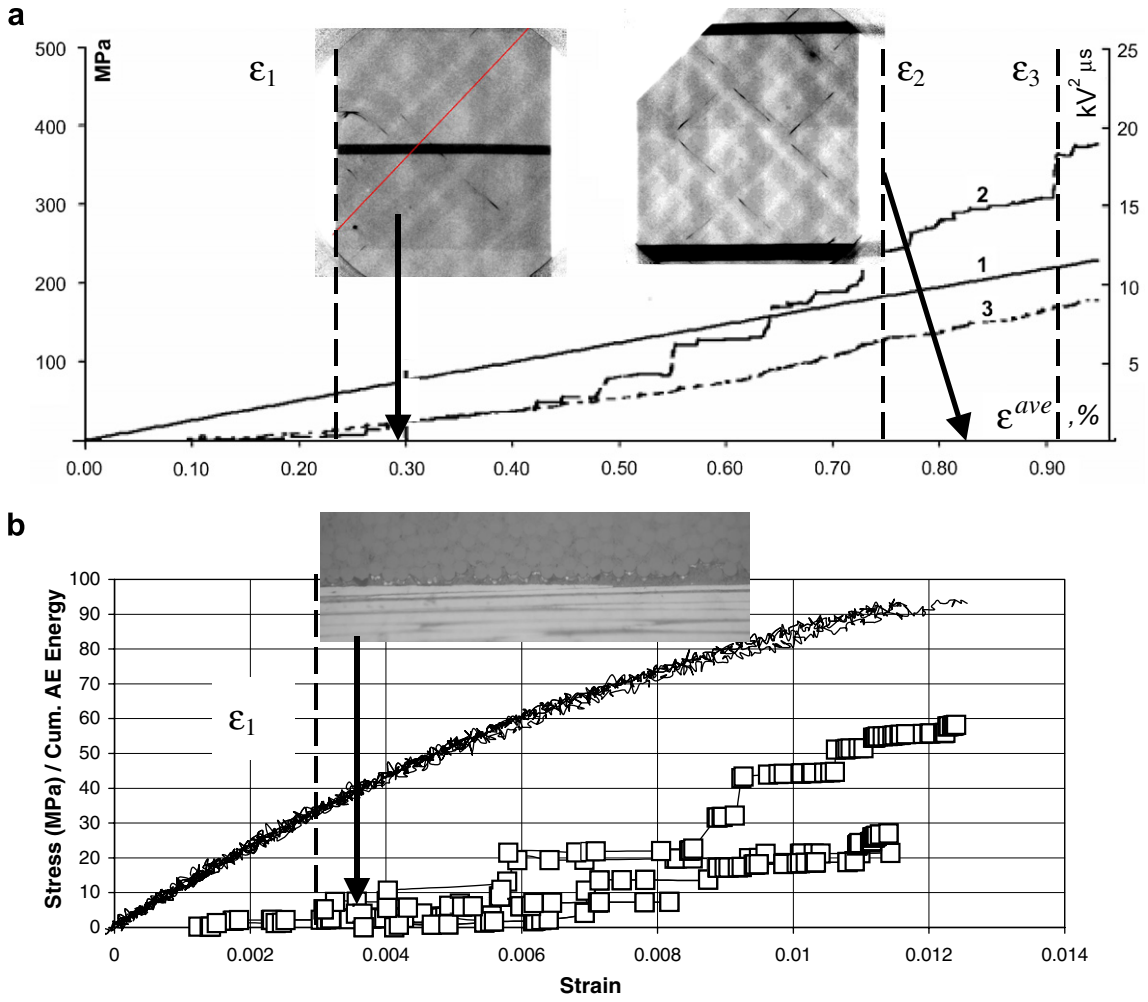

Fig. 3. Stress–strain diagrams and AE registration for carbon/epoxy composites: (a) triaxial braided composite, MD test, 1 – stress–strain diagram, 2 – cumulative AE events energy, 3 – cumulative AE event count, insets – X-ray images; (b) quasi-UD woven composite, 30° test direction, combined results of five tests, lines – stress–strain diagrams, points – cumulative AE event energy, inset – microscopy showing early delamination between carbon and glass yarn.

Table 2
Characteristic strain levels, %

Material	Test direction	ε_1	ε_2	ε_{ult}
3-axial braid	MD	0.29	0.55	1.45 ± 0.15
	BD	0.36	0.45	1.25 ± 0.18
	CD	0.33	0.43	1.11 ± 0.03
Quasi-UD	0°	0.16	n/a	2.25 ± 0.058
	30°	0.4	n/a	1.79 ± 0.28
	45°	0.4	n/a	1.08 ± 0.23
	60°	0.4	n/a	1.00 ± 0.26
	90°	0.15	n/a	0.80 ± 0.25

Table 2 lists the characteristic strain levels for the studied materials and different test directions.

5. Damage development

With the characteristic strain levels identified, the damage investigation proceeds further to studying the damage structure under loading up to the characteristic levels. This is done using non-destructive techniques: Ultrasonic C-scan (not considered here, see [22]) and X-ray investigation, and then doing microscopy at the sections made on the sites identified by the X-ray investigation. The typical results of such a study are illustrated in this section for the two materials under consideration. These two examples demonstrate two types of damage initiation: by transverse cracking and by shear-induced local delaminations.

5.1. Triaxial braided composite

Figs. 4 and 6 demonstrate the development of cracks in triaxial braided composite. The crack structure is clearly revealed by X-ray images and is further investigated by microscopy of the cross-sections.

Transversal cracks in the yarns, with the plane oriented in the direction of the yarns, start developing at ε_1. The cracks are confined in one ply/one yarn, being therefore limited in width as well as in length. When two yarns with the same direction of the fibres are in contact, a crack can

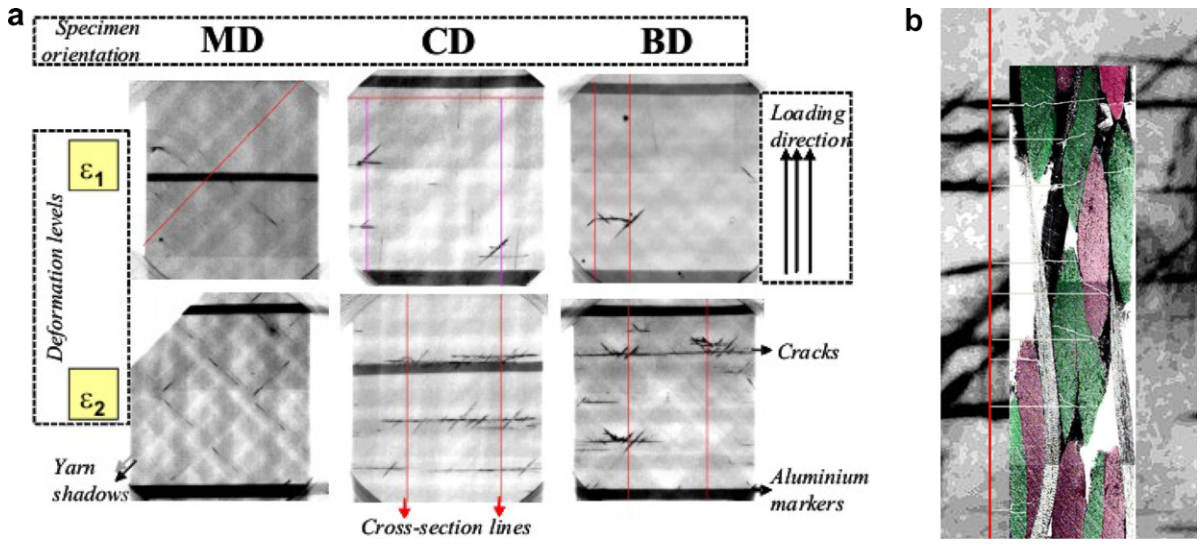

Fig. 4. Damage in triaxial braided carbon/epoxy composites: (a) X-ray images of the crack patterns for two strain levels (see Table 2); (b) cross-section of a specimen loaded in BD up to ε_2 strain level.

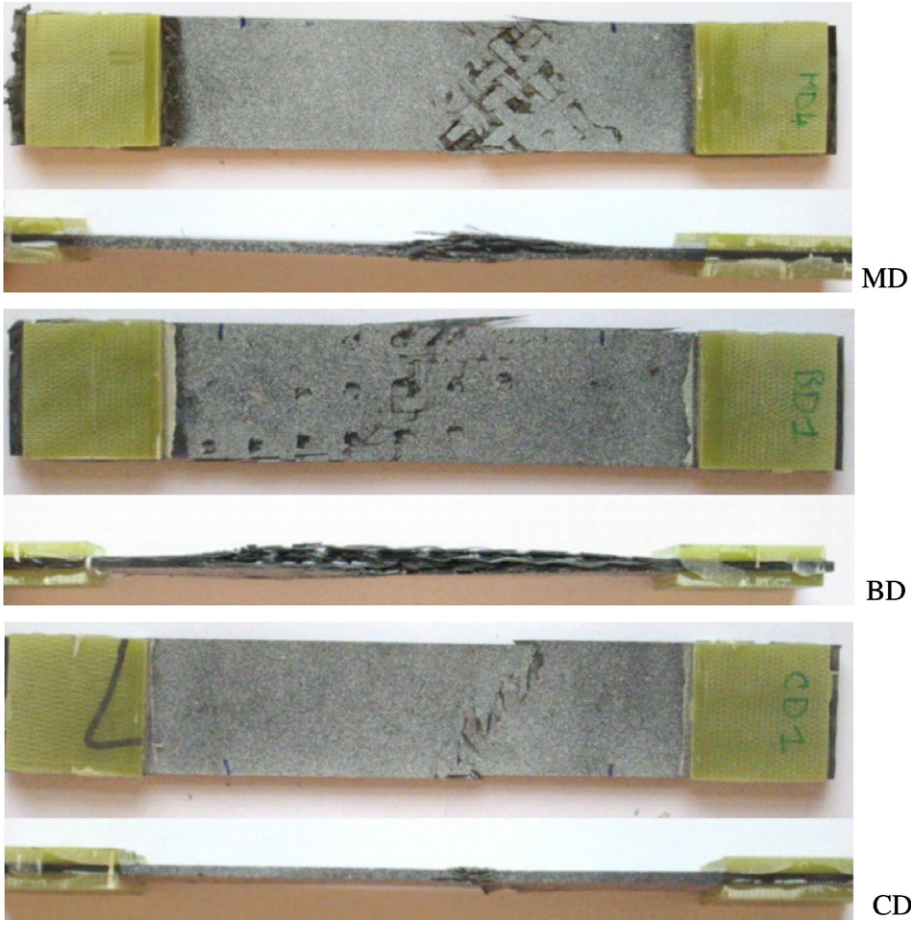

Fig. 5. Triaxial braided carbon/epoxy composite samples after final failure.

travel from one yarn to another. FE modelling, reported in detail in [11,20] shows that these cracks are caused either by transversal tension or shear strains. With the increase of strain the cracks multiply, the length increases (Fig. 6). Longer cracks are developed in the yarns which are oriented at 90° to the loading direction, but these cracks still

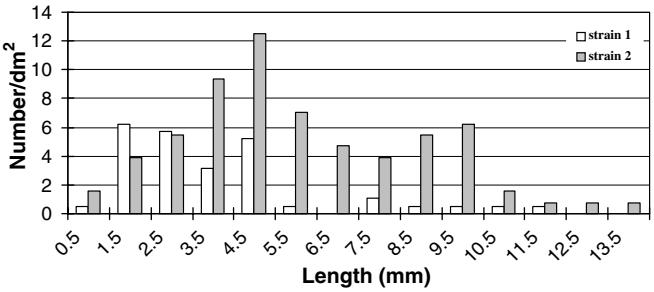

Fig. 6. Distribution of the crack length in triaxial braided carbon/epoxy composite loaded in MD for ε_1 and ε_2 strain levels (see Table 2).

have limited length and do not go from one end of the sample to another. At the strain level ε_2 local delaminations start, as shown in Fig. 2.

The samples final failure for MD and BD tests (in the direction of inlays and braiding yarns correspondingly) is delamination and consecutive fibre breakage (Fig. 5). Straightening of highly crimped braiding yarns produce out-of-plane stresses with create large delamination zones. This delemination zones are smaller for samples tested in MD, as the inlay yarns are less crimped. Off-axis CD loading leads to more localized fracture locus coinciding in the direction and width with the braiding yarns.

5.2. Quasi-UD woven composite

In spite of clear detection of acoustic events over ε_1 threshold, X-ray examination of samples after tensile test up to this strain level did not show any cracks in the samples, apart from 90° tests, where transversal cracks were revealed. To determine the source of AE activity and stiffness degradation, optical microscopy was used. The cross-sections of the samples (made in two directions: orthogonal to the carbon warp and glass weft yarns) were observed under 20× and 50× optical magnification. These observation have shown the following (Fig. 7).

Small cracks have formed between the carbon and glass yarns in *only* the surface textile layers within the composite in the off-axis samples. These cracks, surprisingly, are *parallel* to the sample surface. The fact that these cracks are parallel to the force, and are located at or near the carbon–glass interface indicates that these cracks have formed due to shear between the glass and carbon yarns. Fig. 7c shows that the crack runs between the carbon and glass yarns when the glass yarn is on the outside (at the edge of the composite), but when the glass yarn moves under the next carbon yarn, the crack is transferred into the second carbon yarn, and continues there until the next carbon yarn where it resumes its place between the glass and carbon yarns. This transfer of the crack across the glass yarn is accomplished without breaking the glass yarn itself.

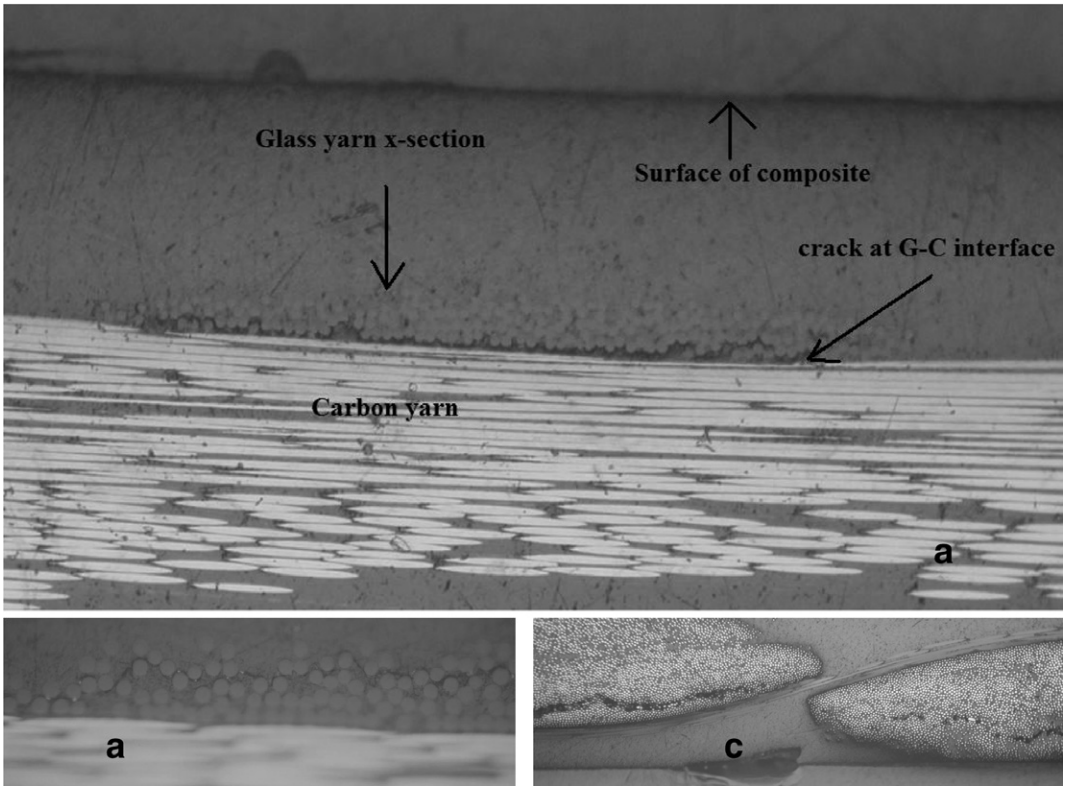

Fig. 7. Cracks in carbon/epoxy woven quasi-UD composite, load direction 30°: (a) crack formed in the surface layer; (b) magnified image of the same crack; (c) crack follows the glass–carbon interface when the glass yarn is at the outside; when the glass yarn moves over another carbon yarn, the crack continues through the carbon.

Please cite this article in press as: Lomov SV et al., Experimental methodology of study of damage initiation ..., Compos Sci Technol (2007), doi:10.1016/j.compscitech.2007.07.005

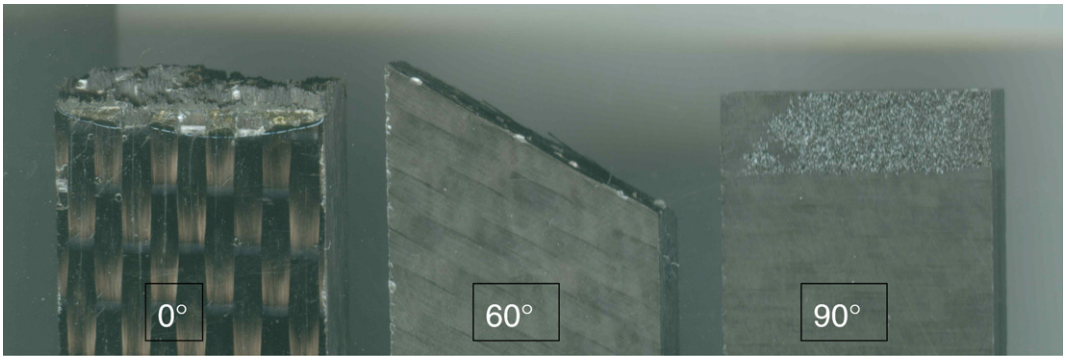

Fig. 8. Carbon/epoxy woven quasi-UD composite samples after final failure.

Table 3
"Road map" of the experimental study of damage in textile composites

Tests/data analysis	Data
Textile preparation/shearing, impregnation, measurements of yarn shapes, local Vf	Geometric characterisation of the reinforcement in composite
X-ray on unloaded samples	Thermal/cure damage characterisation
Tension tests with AE and full-field registration of strains	Tension diagrams; strain maps AE diagrams
Identification of characteristic strain levels ε_1, ε_2, ε_{ult}	Damage initiation threshold
Tensile tests till characteristic strain levels ε_1, ε_2, ε_{ult}	Damaged samples for further inspection
Ultrasonic C-scan of the damaged samples	Damage extend and periodicity
X-ray inspection of the damaged samples	Cracks placement, orientation, length distribution
Cutting samples for micro-inspection according to the crack placement and micrography	Fine structure of damage
Scanning electron microscopy (SEM)	Micro-characterisation of damage

The glass interlacing yarns are very thin and are sparsely distributed in the textile, and the cracks generated in the material only seem to occur when there is an interaction (overlapping) between the carbon and the glass yarns at the surface. Therefore, the size of the defects is small and they are generally not connected to the surface and were not readily observable using X-ray.

The samples tested in the fibre direction (0°) fail by fibre failure (Fig. 8). Other test directions (30°, 45°, 60° and 90°) produce clear shear/transversal failure along the fibres.

6. Conclusions

We have outlined an experimental methodology for study of initiation and development of damage in textile composites in tension test. The test "road map" is summarised in Table 3. The methodology has been applied to different textile composites: carbon/epoxy triaxial braids, quasi-UD woven, NCF (reported elsewhere [22,23,26]). The methodology is based on identification of the characteristic levels of the applied load. These levels are further used for investigation of damage modes and crack structure in the material. The same levels could be further used for planning of experiments under other types of loading, including fatigue [31,32].

Acknowledgements

The work reported here has been carried out in the scope of the projects TECABS, ITOOL (European Commission), "Predictive tools for permeability, mechanical and electromagnetic properties of fibrous assemblies" (IWT, Flanders) and PhD grant of K.U.Leuven Research Council (D.S. Ivanov). The paper includes results of Master theses of F. Baudry, K. Vander Bosch, H. Xie in Master of Materials Engineering program in Department MTM, K.U.Leuven.

References

[1] Bogdanovich AE. Multi-scale modeling, stress and failure analyses of 3D woven composites. J Mater Sci 2006;41(20):6547–90.
[2] Bogdanovich AE, Pastore CM. Mechanics of textile and laminated composites. London: Chapman & Hall; 1996.
[3] Bogdanovich AE, Pastore CM. Material-smart analysis of textile-reinforced structures. Compos Sci Technol 1996;56:291–309.
[4] Lomov SV, Huysmans G, Luo Y, Parnas R, Prodromou A, Verpoest I, et al. Textile composites: modelling strategies. Composites Part A 2001;32(10):1379–94.
[5] Verpoest I, Lomov SV. Virtual textile composites software Wisetex: integration with micro-mechanical, permeability and structural analysis. Compos Sci Technol 2005;65(15–16):2563–74.
[6] Zako M, Uetsuji Y, Kurashiki T. Finite element analysis of damaged woven fabric composite materials. Compos Sci Technol 2003;63:507–16.
[7] Fish J, Yu Q. Two-scale damage modeling of brittle composites. Compos Sci Technol 2001;61:2215–22.
[8] Karkkainen RL, Sankar BV. A direct micromechanics method for analysis of failure initiation of plain weave textile composites. Compos Sci Technol 2006;66:137–50.
[9] Tang X, Whitcomb JD. Progressive failure behaviour of 2D woven composites. J Compos Mater 2003;37(14):1239–59.
[10] Greve L, Pickett AK. Modelling damage and failure in carbon/epoxy non-crimp fabric composites including effects of fabric pre-shear. Composites Part A – Appl Sci Manufact 2006;37(11):1983–2001.

[11] Lomov SV, Ivanov DS, Verpoest I, Zako M, Kurashiki T, Nakai H, et al. Meso-FE modelling of textile composites: road map, data flow and algorithms. Compos Sci Technol 2007;67:1870–91.
[12] John S, Herszberg I, Coman F. Longitudinal and transverse damage taxonomy in woven composite components. Composites Part B 2001;32:659–68.
[13] El Hage C. Modelisation du comportement elastique endommageable de materiaux composites a renfort tridimensionel. Laboratoire Roberval. Compiegne: L'Universite de Technologie de Compiegne; 2006.
[14] Kurashiki T, Zako M, Verpoest I. Damage development of woven fabric composites considering an effect of mismatch of lay-up. In: Sol H, Degrieck J, editors. Composites for the future, Proceedings of the 10th European conference on composite materials (ECCM-10); 2002 [CD edition].
[15] Uetsuji Y, Zako M, Nishiyabu K. Numerical analysis and in-situ SEM observation of damage development for woven fabric composite materials. J Soc Mater Sci – Jpn 2002;51(10):1147–53.
[16] Sugimoto K, Nakai A, Hamada H. Effect of lamination sequence on mechanical behaviour of woven composites, In: Proceedings of the 7th international conference on textile composites (TexComp-7); 2004. p. 1–4 [Textile 22].
[17] Masters JE, Ifju PG. A phenomenological study of triaxially braided textile composites loaded in tension. Compos Sci Technol 1996;56(3):347–58.
[18] Ivanov DS, Lomov SV, Verpoest I, Zisman AA. Noise reduction of strain mapping data and identification of damage initiation of carbon-epoxy triaxial braided composite. In: Camanho PP, Wisnom MR, Pierron F, editors. Composites testing and model identification (CompTest-2006); 2006 [CD edition].
[19] Ivanov DS, Lomov SV, Verpoest I, Baudry F, Xie H. Damage initiation and development in triaxial braid and fine structure of damage. In: Proceedings of the European conference on composite materials (ECCM-12), 29th August–1st September; 2006 [CD edition].
[20] Ivanov DS, Lomov SV, Verpoest I, Zako M, Kurashiki T, Nakai H, Hirosawa S. Meso-FE modelling of 3-axial braided composites. In: Proceedings of the 8th international conference on textile composites (TexComp-8); 2006 [CD edition].
[21] Edgren F, Mattsson D, Asp LE, Varna J. Formation of damage and its effects on non-crimp fabric reinforced composites loaded in tension. Compos Sci Technol 2004;64:675–92.
[22] Truong Chi T, Vettori M, Lomov SV, Verpoest I. Carbon composites based on multiaxial multiply stitched preforms. Part 4: Mechanical properties of composites and damage observation. Composites Part A 2005;36:1207–21.
[23] Truong Chi T, Chiew Jie H, Lomov SV, Verpoest I, Sheared biaxial multi-ply carbon fabrics reinforced epoxy composites: the mechanical properities and damage initiation, Proceedings 26th SAMPE-Europe Conference, Paris, 5th–7th April; 2005. p.252–57.
[24] Asp LE, Edgren F, Sjögren A. Effects of stitch pattern on the mechanical properties of non-crimp fabric composites. In: Proceedings of the ECCM-11; 2004 [CD Edition].
[25] Mattsson D, Joffe R, Varna J. Methodology for characterization of internal structure parameters governing performance in NCF composites. Composites Part B – Eng 2007;38(1):44–57.
[26] Mikhaluk DS, Truong TC, Borovkov AI, Lomov SV, Verpoest I. Experimental observations and finite element modelling of damage and fracture in carbon/epoxy non-crimp fabric composites. Eng Fract Mech, [in print].
[27] Mattsson D, Joffe R, Varna J. Damage in NCF composites under tension. Eng Fract Mech, [in print].
[28] Wevers M, Surgeon M. Acoustic emission and composites. In: Kelly A, Zweben C, editors. Comprehensive composite materials. Elsevier; 2000. p. 345–57 [chapter 5.14].
[29] Benmedakhene S, Kenane M, Benzeggagh ML. Initiation and growth of delamination in glass/epoxy composites subjected to static and dynamic loading by acoustic emission monitoring. Compos Sci Technol 1999;59:201–8.
[31] Vallons K, Zong M, Lomov SV, Verpoest I. Carbon composites based on multi-axial multiply stitched preforms. Part 6: Stiffness degradation and tensile strength evolution during fatigue. Composites Part A, [in print].
[32] Vallons K, Zong M, Lomov SV, Verpoest I. Carbon composites based on multi-axial multiply stitched preforms: stiffness degradation and tensile strength evolution during fatigue. In: Proceedings of the European conference on composite materials (ECCM-12), 29th August–1st September; 2006 [CD edition].

Please cite this article in press as: Lomov SV et al., Experimental methodology of study of damage initiation ..., Compos Sci Technol (2007), doi:10.1016/j.compscitech.2007.07.005